

Lawrence Berkeley National Laboratory

Recent Work

Title

MEASUREMENT OF THE PRODUCT MASS DISTRIBUTIONS FROM HEAVY-ION-INDUCED NUCLEAR REACTIONS, I: GAMMA-RAY SPECTROMETRIC PRODUCT IDENTIFICATION

Permalink

<https://escholarship.org/uc/item/9kt18966>

Author

Morrissey, D.J.

Publication Date

1978-04-01

MEASUREMENT OF THE PRODUCT MASS DISTRIBUTIONS FROM
HEAVY-ION-INDUCED NUCLEAR REACTIONS,
I: GAMMA-RAY SPECTROMETRIC PRODUCT IDENTIFICATION

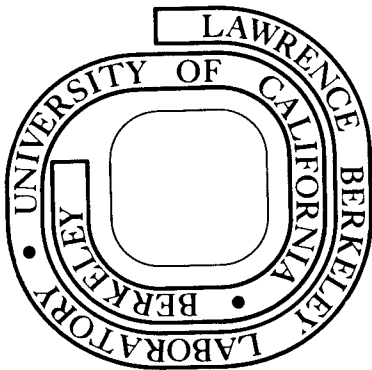
D. J. Morrissey, D. Lee, R. J. Otto, and G. T. Seaborg

April 1978

RECEIVED
LAWRENCE
BERKELEY LABORATORY

AUG 22 1978

LIBRARY AND
DOCUMENTS SECTION
Prepared for the U. S. Department of Energy
under Contract W-7405-ENG-48



TWO-WEEK LOAN COPY

This is a Library Circulating Copy
which may be borrowed for two weeks.
For a personal retention copy, call
Tech. Info. Division, Ext. 6782

e.2
LBL-7711

DISCLAIMER

This document was prepared as an account of work sponsored by the United States Government. While this document is believed to contain correct information, neither the United States Government nor any agency thereof, nor the Regents of the University of California, nor any of their employees, makes any warranty, express or implied, or assumes any legal responsibility for the accuracy, completeness, or usefulness of any information, apparatus, product, or process disclosed, or represents that its use would not infringe privately owned rights. Reference herein to any specific commercial product, process, or service by its trade name, trademark, manufacturer, or otherwise, does not necessarily constitute or imply its endorsement, recommendation, or favoring by the United States Government or any agency thereof, or the Regents of the University of California. The views and opinions of authors expressed herein do not necessarily state or reflect those of the United States Government or any agency thereof or the Regents of the University of California.

MEASUREMENT OF THE PRODUCT MASS DISTRIBUTIONS FROM
HEAVY-ION-INDUCED NUCLEAR REACTIONS,
I: GAMMA-RAY SPECTROMETRIC PRODUCT IDENTIFICATION

D. J. Morrissey, D. Lee, R. J. Otto, and G. T. Seaborg

Lawrence Berkeley Laboratory and Department of Chemistry
University of California
Berkeley, California 94720

ABSTRACT

A system for the measurement of the product mass yield distributions from heavy-ion-induced nuclear reactions has been developed. This system is based on the gamma-ray spectrometric identification of product radioactivities in the irradiated target materials or in separated chemical fractions derived from the target. Gamma-ray spectra are collected as a function of time and all peaks and peak areas are identified and measured with a modified version of SAMPO. Decay curves for all gamma-rays observed in two or more spectra are constructed by the computer code TAU1. A current table of all the known gamma-ray transitions is then used to match a known gamma-ray energy and half-life to each measured decay curve. This is done interactively with the computer code TAU2 and a Tektronix graphics terminal. Examples of the various options are given. Nuclear reaction cross-sections are calculated on weighted average of all the observed gamma-rays for each product nuclide after the identifications have been screened for duplicate or erroneous identifications and for self-consistency.

1. INTRODUCTION

Gamma-ray spectrometric methods have been developed to deduce mass yield distributions for heavy-ion-induced nuclear reactions at incident particle energies ranging from 5.0 MeV/A to 8.5 MeV/A and 0.4 to 2.1 GeV/A. These nuclear reactions produce radioactive, gamma-ray emitting, nuclides that cover the entire chart of the nuclides. In a single heavy-ion reaction such as ~ 960 MeV $^{136}\text{Xe} + ^{238}\text{U}$ [1] or 25.2 GeV $^{12}\text{C} + ^{238}\text{U}$ [2] over 100 neutron-excessive and neutron-deficient nuclides ranging from ^7Be to ^{238}Np were produced and identified by their characteristic gamma-ray transitions between 90 keV and 2 MeV by spectrometric measurements of the target activities.

The object of the analysis is to translate the complicated gamma-ray spectra resulting from gamma-ray spectroscopy of irradiated foils into a data set consisting of the partial cumulative and independent yield production cross sections from which isobaric mass yield distributions can be deduced. In the development of a computer aided interactive analysis system, the following criteria were established.

- a. The energy resolution and the linear and differential stability of the gamma-ray spectrometer system should be excellent. System resolutions on the order of 2.0 keV FWHM for the ^{60}Co 1332 keV gamma-ray were obtained and the linear stability of the systems was maintained for periods ranging over several months. We also require a system in which the photopeaks are nearly Gaussian in shape and unchanging with time. The efficiency of the detector system has to be well known for the many counting geometries that are used during spectrometric measurements of different chemical fractions from a single target.
- b. Given the above energy stability and photopeak shape requirements, the counting geometry and counting schedule should be adjusted so that production cross section information can be obtained on the greatest number of nuclides, and therefore, the gamma spectroscopic measurements should span the largest range of half-lives possible.

- c. All routine data handling and processing should be made completely automatic. This includes data acquisition, photopeak analysis and preparation for an interactive decay half-life analysis.
- d. In those areas of analysis where a large number of factors must be considered, such as in the assignment of known γ -ray transitions to the measured decay curves of the observed gamma rays, the system should be an interactive one. It is at this point, also, that the experimenter should be able to evaluate the quality of the data and be able to recognize readily any systematic errors that the previous automatic part of the analysis may have introduced.

The first criterion above can be met with many commercially available systems today and this aspect will be discussed only briefly. With respect to the second criterion, a counting strategy has been developed that takes into account first, the problem of high count rate distortions of the peak shape associated with a very radioactive target that is continuously decaying, and second, the wide range of half-lives of the gamma-ray emitting products in the target. The identification and analysis of photopeaks in the spectra is done with a modified version of the program SAMPO [3]. The modified automatic mode of this program, which was written for the CDC-7600 machine at the Lawrence Berkeley Laboratory, has proven to be very successful. The many desirable features of this program that have made it possible to detect reliably and automatically over 100 photopeaks in a single 4000-channel spectrum and to calculate their associated decay rates in the target will be discussed from the perspective of this somewhat unique task.

Possibly more significant and certainly more important to the analysis system that we have developed is the interactive graphics display program, TAU2, which makes it possible to identify reaction products based on their half-lives

and known gamma-ray transitions. The present system displays the energy and decay curve for a single gamma-ray identified in a series of spectra, along with pertinent information on those isotopes which have a gamma-ray transition with the same or nearly the same energy. Each list of candidate isotopes is derived from an updated abridged compilation by Binder et al.[4] of the MacMurdo-Bowman tables [5]. Although this interactive program is presently run on the CDC-6000 series machines with a Tektronix 4014 Terminal at LBL, it could easily be adapted to a smaller computer such as the PDP-11. It is at this point that an experimenter can readily spot systematic errors in the analysis and determine the quality of the data set. Once a set of partial cumulative and independent-yield cross sections are obtained an iterative procedure is used to deduce the mass and charge distribution for the nuclear reaction under study. The analysis scheme that we have developed is shown schematically in Figures 1A and B.

In Section 2 we describe the gamma-ray spectrometers that have been used and their calibration. Section 3 discusses the use of the code SAMPO for the analysis of the complex gamma-ray spectra generated for each experiment. The interactive computer graphics half-life identification of the observed gamma rays is contained in Section 4. The origins of errors and their treatment is covered in Section 5, and the calculation of the final cross sections in 6.

2. EXPERIMENTAL CONDITIONS AND INSTRUMENTAL CALIBRATION

In general there are two classes of experiments, and therefore gamma-ray samples, that have been employed to study heavy-ion-induced nuclear reaction products. The first experiment with a given heavy-ion target system is generally the irradiation of a thick target foil followed by direct gamma-ray spectroscopy

of the target. The systems studied by this method have ranged from ~ 224 MeV $^{48}\text{Ca} + 0.25\text{-mm-thick natural silver target}$ [6] to 25.2 GeV $^{12}\text{C} + 72$ mg/cm² natural uranium [2]. The initial β - γ radiation from these targets ranged from a few tens to a few hundred mr/hr-cm² at ~ 10 cm.

The second type of experiment involves the irradiation of a thick target followed by chemical separation of the product radioactivities. The chemical separation scheme most often used with uranium targets by our group has been described elsewhere [7]. Chemical separation of the product radioactivities allows a more careful study of reaction products with low cross-sections that are not observable in the direct spectroscopy experiments. The samples generated by the chemical separations have ranged from AgI/AgBr precipitates on a cellulose filter to a few milliliters of eluent in a glass vial from column chromatographic separations [8].

All gamma-ray spectrometric measurements are made with three ORTEC coaxial Ge(Li) diodes with a nominal 60 cm³ active volume and a "right-angle" geometry. The samples are mounted on aluminum cards which are held rigidly in lucite holders attached to the Ge(Li) detectors. These holders were machined to reproducibly hold the sample cards in approximately 14 known geometries relative to each detector. These geometries spanned source-detector separations of between ~ 14 and ~ 1 cm. A given sample was generally measured with only one detector. Each detector, sample, and lucite sample rack is contained in a shield of volume ~ 1 m³ to reduce contributions to the spectra from γ -ray background activity and contributions from backscattering. The shield consisted of 5 cm of lead, 0.3 cm steel and 0.3 cm aluminum. A standard graded shield of lead, cadmium and copper was not used due to the high cost of materials needed for a one-cubic-meter volume shield and because photons with energies

less than 90 keV, such as lead x rays, were excluded from the spectra by a lower level discriminator.

Signals arising in the Ge(Li) detector were fed into an ORTEC charge-sensitive preamp (Model #120-4) and then into a high-rate linear amplifier. The output rise time of the high-rate amplifier was matched to the input specifications of a 100 megahertz Northern Scientific ADC. This ADC was part of a pulse height analysis system that included a Texas Instruments TI-960A minicomputer and an Ampex magnetic tape drive. This system was originally designed to collect a single 4096-channel spectrum along with a 40-character identifier and output them on magnetic tape. Subsequently a real time clock with a Julian calendar readout was added to enable the system to record the real time start and stop points of each measurement on the magnetic tape with each spectra.

2.1 Energy Calibration of Systems

All calibrations of the systems were performed with a National Bureau of Standards standard reference material gamma-ray source, SRM-4216-C [9]. This is a mixed radionuclide, essentially windowless, point source that can be used for energy as well as for efficiency calibration of high resolution gamma-ray detectors. A list of the nuclides and their radiations used in the energy calibration of the Ge(Li) detectors is given in Table I. The energy calibration was made by least squares fitting the centroids of the known energy gamma-ray peaks as determined by SAMPO [3] (see below) to a third order polynomial of the form:

$$E_{\gamma} = \sum_{i=1}^4 a_i (\text{channel no.})^{i-1} \quad (1)$$

TABLE I. National Bureau of Standards mixed-radionuclide gamma-ray emission-rate point-source standard reference material, SRM-4216-C.

Gamma ray energy (keV)	Nuclide	Half-life
88.03	^{109}Cd	453 days
122.06	^{57}Co	270 days
136.47	^{57}Co	270 days
165.8	^{139}Ce	137 days
279.21	^{203}Hg	36.7 days
391.7	^{113}Sn	115 days
513.98	^{85}Sr	65.2 days
661.64	^{137}Cs	30.1 years
898.0	^{88}Y	106 days
1173.21	^{60}Co	5.26 years
1332.48	^{60}Co	5.26 years
1836.1	^{88}Y	106 days

The polynomial in centroid channel number was least squares fit to the known energies of the standard gamma-rays with the least squares routine contained in SAMPO [3]. Contributions from the the second and third degree polynomial terms can be seen in Fig. 2 where the difference between a linear fit to the calibration data and a third degree polynomial fit is plotted versus channel number.

The resolution of the entire spectrometric system was also measured with the SRM-4216-C standard. The resolution of a Ge(Li) spectrometer is traditionally quoted in terms of the FWHM of the ^{60}Co 1332.5 keV gamma-ray peak; these values, as well as additional resolution information, are contained in Table II. With the exception of Ge(Li)-1, the system resolutions are excellent. The poor resolution of this latter detector limited its usefulness to measurements of relatively simple gamma-ray spectra, e.g. radiotracer chemical yield determinations, and it was not used for spectroscopy of irradiated targets.

2.2 Efficiency Calibration of Systems

All the efficiency calibrations were performed with the NBS standard SRM-4216-C by comparing the known gamma-ray emission rates with those measured as a function of both geometry and energy. The energy dependence of the efficiency, ϵ_{γ} , of Ge(Li) gamma-ray detectors has been postulated to have the form [10]:

$$\epsilon_{\gamma}(E_{\gamma}) = P_1 [E_{\gamma}^{P_2} + P_3 \exp(P_4 E_{\gamma})] \quad (2)$$

The efficiency of each Ge(Li) spectrometer system was measured and the four coefficients in equation (2) were obtained by least squares fitting the observed intensities to those expected as a function of energy for all the possible

TABLE II. System resolution characteristics. Measured FWHM in keV.

Detector	^{57}Co 122.1 keV	^{137}Cs 661.6 keV	^{60}Co 1332.5 keV
Ge(Li)-1	2.21	2.49	2.92
Ge(Li)-2	1.28	1.60	2.00
Ge(Li)-3	1.37	1.69	2.05

source-detector geometries. A set of such efficiency curves for the Ge(Li)-3 system is shown in Fig. 3.

Another source of error that becomes important with strong radiation sources is loss from the photopeak* through coincident summing of detector pulses. The seriousness of the summation of random coincident gamma-rays is dependent on the resolving time of the system and is thus related to the count rate. We have determined that the loss of photopeak efficiency due to random summing was insignificant for count rates below 3×10^5 counts/min; and for count rates above 9×10^5 c/min the loss was about 8 percent. For those radio nuclides which emit two or more gamma rays in cascade following β -decay, the summing loss, due to the true coincidence in the decay, is dependent on the source-detector geometry. Fig. 4 shows the photopeak sum as a function of geometry for the two gamma-ray cascade that occurs in the decay of the radionuclide ^{94}Nb . The measurements were made at count rates at which random coincident summing could be neglected. In view of these limitations of the spectrometer systems, samples were not positioned closer than 3 cm to the detector face and count rates did not exceed $\sim 5 \times 10^5$ counts/min.

2.3 Peak Shape Calibration

An attractive feature of the peak fitting routine in SAMPO is the inclusion of a calibration of the lineshape of the photopeak as a function of the photopeak energy.^{3,10} This is accomplished through the use of a functional form that can be linearly fit to the photopeak energy. The lineshape is taken to be the sum of a Gaussian plus two independent exponential tails smoothly joined to the

*The term photopeak is used here to describe only the full energy peak.

Gaussian, one on the high side and one on the low side. This lineshape can be described by four parameters, the center of the Gaussian, its width, parameter, and the two distances from the center that the exponentials join the Gaussian. The parameters for each of the gamma-ray lines in the SRM-4612-C standard are obtained through the least squares fitting routine in the code and stored on punched cards. The code generates the lineshape parameters for any other part of the spectrum by linear interpolation between calibration points. In figure 5 we have plotted the values the full-width at half-maximum as a function of gamma-ray energy for the SRM-4612-C standard. Also shown is a least square linear fit to the data of the form, $FWHM = mE_{\gamma} + b$. The correlation coefficient, r^2 , of this fit is 0.9988, indicating the validity of the linear interpolation used in SAMPO.

Serious deterioration of the photopeak lineshape was observed at high count rates. This deterioration took the form of increased exponential tailing and a general increase in the asymmetry of the lineshape. However, this deterioration only begins to be apparent at count rates where coincident summing losses are important (see above). Thus, when the count rate was adjusted to minimize coincident summing losses the photo-peak lineshapes were essentially independent of count rate. Also, noting that the gamma-ray efficiency of systems was highest in the region of ~ 100 keV, the large number of K x-rays emitted by irradiated target materials, and the limitations on count rate imposed by our detection system, a lower level discriminator was set at the ADC to eliminate all photons with energies of ~ 90 keV and below.

2.4 Strategies of Radioactivity Measurements

Several strategies of how to schedule the measurements of samples generated by a bombardment have evolved. Empirically determined, the most desirable

situation is one in which two identical targets are irradiated consecutively. The first irradiation should be "short" (~15 minutes) with as high a flux as possible, the second irradiation should be "long" (~hours). This allows the preferential observation of those product activities with short (≤ 30 min) half-lives in the first target while the second target is being irradiated, and then the observation of long-lived ($T_{1/2} \geq 1$ hour) product activities in the second target. Because of the large number of radioactivities observed and their wide range of half-lives, the length of bombardment and scheduling of measurements must be based on average properties of the product radionuclides. Thus, irradiations tailored for specific radionuclides or only even specific half-lives are generally not feasible.

The duration of each measurement of a given sample is dependent on many factors. Binder has considered these factors and has developed a criterion for scheduling samples [11]. The basis of the schedule lies in recognizing that (1) the activities that are observable in the gamma-ray spectrum from a given sample obviously vary with time; and (2) given that all the cross-sections observed in these studies lie between ~ 1 mb and 100 mb, i.e. in a narrow range, there is an optimal period in which to observe an activity with a given half-life. Thus for a single sample, typically the first target described above, the first measurements would be for 2.5 minutes each plus dead time, and then the interval would be doubled to 5 minutes for the next three measurements, and so on. In practice, this was repeated until the length of the measurement was 24 hours, which was usually the longest measurement period. However, measurements have lasted up to ~ 7 days when the identification of specific, long-lived, nuclides was important.

In the more frequent case where more than one sample needed to be measured during a limited time period, one of two options was chosen. For three or less samples the

above schedule was followed and the sample with the most complex gamma-ray spectra received the most measurements. When a target was chemically separated before analysis, five samples were typically generated. Here the samples were counted in a cycle so that the length of time for each cycle was about the length of time after bombardment, divided by the number of samples in the cycle. Again, given samples were generally not measured for longer than 24 hours. Throughout these measurement schedules the geometry of the sample with respect to the detector was adjusted to maintain the ADC dead time at $\lesssim 15$ percent ($\sim 2 \times 10^5$ cpm). As the samples became weaker they were moved closer to the detector with the limiting conditions being dictated by the coincident summing problem previously discussed.

3. SPECTRAL ANALYSIS

The gamma-ray spectra are prepared for the SAMPO analysis by individual screening for energy calibration drift and for correctly recorded start and stop time information. Typically, approximately 25 spectra will be measured for each sample, but this value varies widely with experimental conditions and complexity. The largest number of spectra was approximately 40 when a single target was irradiated and counted by itself. The smallest came from a chemical separation of a target into ~ 5 fractions that were rotated in with ~ 4 unseparated target foils. In this experiment a total of ~ 150 spectra were collected, with the unseparated targets getting ~ 20 measurements each and the chemical fractions somewhat less.

A typical gamma-ray spectrum is shown in Fig. 6. The spectrum is from the direct measurement of a thick gold target that had been irradiated with 1140-MeV ^{136}Xe ions [11]. The spectrum was collected for 5 minutes starting approximately

20 minutes after the end of bombardment. This figure shows that the gamma rays for individual transitions appear as peaks riding on a large, but typically smoothly varying Compton continuum.

3.1 Use of SAMPO

All peak area fitting is done with an automatically operating version of SAMPO. This computer code takes the spectral input on magnetic tape and processes each spectrum individually to determine the energy that corresponds to the centroid as well as the area of all peaks above a controllable significance level. The code outputs this information on magnetic tape for the half-life analysis, as well as a microfiche record of the fit obtained for each peak. SAMPO was chosen for the peak fitting because it contained several attractive features. One very important aspect of the peak fitting is the ability to "calibrate" the lineshape of a peak generated by a gamma-ray spectrometer. In SAMPO the lineshape used to fit peaks contains a central Gaussian and an exponential tail joined smoothly on each side [3], which can be adjusted via a least squares fitting to the exact line shape of the spectrometer. A second attractive feature of this code is that the code was developed to analyze "complex" spectra and as such has included the option of a smoothly varying polynomial-type background continuum.³ This type of background approximation is particularly well suited to the spectra we have to analyze, as can be seen in Fig. 6. Also the ability to run the program in an interactive mode to control the fitting of multiplets is a very useful feature.

The automatic SAMPO analysis is run after the entire system has been calibrated for energy, efficiency, and line shape, and the input spectra have been screened for the pertinent information. The code first reads the calibration

parameters and then cycles through the input spectra one at a time. The code performs three different operations on each spectrum: PEAKFIND, where the code identifies all the peaks in the spectrum; FITDO, which fits the previously calibrated lineshape function to each peak; and RESULTS, where the peak acceptance criterion are applied and those peak areas which survive are output.

SAMPO uses a peak search algorithm based on the method of second-differences [3,10]. The second differences are calculated for each channel and compared with a given threshold value. The significance of the second difference is written $SS_i = dd_i/sd_i$, where the second difference dd_i in Channel i is,

$$dd_i = \sum_{j=-k}^{+k} C_j N_{(i+j)}, \quad (3)$$

and its standard deviation

$$sd_i = \left\{ \sum_{j=-k}^{+k} C_j^2 N_{(i+j)} \right\}^{1/2} \quad (4)$$

The coefficients, C_j 's, for the weighting function have the form of the second derivative of a Gaussian, whose width parameter is taken from the shape calibrations. The statistical significance of the second difference is then computed for each channel and it is compared with two input threshold values. The lower of the two defines the potential peaks and the higher defines their acceptance level; these values are normally 2 and 5 respectively. In addition to the computed statistical significance of a potential peak, the accepted peaks also have to pass the peak-shape test. For this test, the number of channels, X_i , whose second-difference values have the same sign as that of the second difference of the peak channel, is compared with the number predicted on the basis of a Gaussian shape for the peak. An acceptable tolerance is ± 2 channels, or

$0.5 X_i$ whichever is larger. The accepted peaks which have passed the above tests are then entered into an array to be least squares fitted. The above present acceptant values have been found to be quite satisfactory for routine analysis.

In order to run SAMPO in this automatic mode, several modifications had to be made to the original code. The input format was changed to read all the pertinent information that describes each spectrum from magnetic tape, i.e. the spectrum tag, the start and stop time of the measurement and the measurement geometry. Any errors on the magnetic tape can be overridden by computer card input. The code was also modified to eliminate most of the input control cards so that the DATAIN control card started the automatic sequence of PEAKFIND, FITDO and RESULTS. And the output was modified to give one record on magnetic tape for each spectrum processed, as well as a microfiche record of the PEAKFIND table, all peak fits, and the RESULTS table. Each record on magnetic tape contained the sample identification, the time after the end of bombardment of the midpoint of the measurement, and the energy, intensity (γ/min , corrected for detection efficiency), and error in the intensity for each peak accepted.

4. INTERACTIVE COMPUTER GRAPHICS HALF-LIFE ANALYSIS

After the spectral analysis is complete, the next step of the process is to sort the observed gamma-ray peak areas so that decay curves can be constructed. The code TAU1 was written to perform this sorting. The code starts with the magnetic tape output from SAMPO and searches both on the spectrum identification tag and on gamma-ray energy. Through the analysis, the time sequence of the original measurement schedule is preserved. That is, the SAMPO analysis was performed in chronological order which TAU1 preserves, thereby eliminating the need for any chronologic sorting in TAU1. The code is able to sort the peak areas

by γ -ray energy from up to 40 spectra for each of 10 samples. The code then generates a new magnetic tape as output that contains the gamma-ray intensities sorted by energy for each of the samples.

The code performs the sorting by first locating the data from the first sample and then the γ -ray with the lowest energy; it then searches for the next measurement of the same sample and checks for a gamma-ray with an energy in an energy window centered on the already established mean energy, \bar{E}_γ . This window has a size Δ that has been described by the empirical equation:

$$\Delta/2 \equiv (\log_{10} \bar{E}_\gamma) - 1.5 \quad (5)$$

This gives an acceptance window of ± 0.5 keV for a 100-keV γ -ray and ± 1.5 keV at 1000 keV. As the code continues its search the mean gamma-ray energy is recalculated after each addition and those peak areas and energies already accepted are removed from the list of future possibilities. After the sorting is complete and all information has been collected for each E_γ , a least squares analysis is performed to give an estimate of the half-life of the gamma-ray. The code also provides a printed output of all the accepted gamma-rays for each sample along with the results of the least square estimate of the half-life and the number of each spectrum in which the gamma-ray was observed.

The next stage of the analysis is to bring the measured decay curves for each γ -ray together with a compilation of the known γ -ray transitions in order to identify the radionuclides present in the sample. For this task we have written the computer code TAU2, which is an interactive decay curve analysis program that constructs decay curves and also presents relevant data on the nearest known γ -ray transitions to facilitate the identification. Twenty γ -ray candidates are displayed at a single time with the option of changing the

list by one candidate at a time. The code has been designed to run on the CDC-6000 series machines at LBL with Tektronix 4014 terminal. Input data for this code is the sorted γ -ray data from TAU1 and a listing of the abridged γ -ray table of Binder et al [4], both on magnetic tape. The code begins with the lowest energy γ -ray observed in the first sample and plots a semilogarithmic decay curve versus time in days on the CRT of the terminal. Simultaneously the code searches the γ -ray table for a known γ -ray transition nearest the averaged measured γ -ray energy. Finding the closest known γ -ray, the code presents the energy, isotope, half life, relative intensity and parents (if any) for the twenty gamma rays nearest the measured energy. The operator is then able to choose any single known line or combination of known lines to be fit to the measured decay curve, or arbitrary half-lives may be fit to the data. The possible combinations are presented in Table III. In all of the options the half lives are held constant and the A_0 values are determined by the least squares routine. When an acceptable identification of the decay curve has been made, the graphics display is recorded on microfiche and the A_0 value along with its error, energy and radionuclide identification is output on a punched card. This A_0 value has units of decays per minute, having been corrected for the abundance of the transition for that nuclide and the branching ratio of the parent nuclide when necessary. A schematic diagram of the code TAU2 is shown in Figure 7.

Typical graphics terminal displays observed in this work are shown in Figures 8, 9 and 10. These figures represent exactly the display that would be presented to the operator as the data analysis is in progress and which is permanently recorded on microfiche. For example, in Fig. 8 the open circles represent the measured decay rate as a function of time for a 159.3 keV gamma-ray. The ordinate is the logarithm of the count rate (in gammas per minute) and the abscissa is the midpoint of the measurement after the end of bombardment, measured in days. The solid curve is the result of least square fitting the operators choice, ^{123}I , to the data. It is interesting to note

that in this case that the identification is essentially unambiguous because of the uniqueness of the ^{123}I half life among gamma-ray transitions in this energy region. Figure 9 presents an example of a two component fit to a gamma-ray line, and figure 10 presents the results from the fitting of the growth and decay of ^{135}Xe to a set of data points.

4.1 Gamma Ray Table

The gamma-ray table used in this work has been published elsewhere [4], but a brief description is in order as it was developed as part of this analysis scheme. The first table that was used for the identification of γ -rays was an original compilation from the literature. This table was merged with the Bowman-MacMurdo table when it became available [5]; and has been subsequently updated as new information became available on specific nuclear decay schemes. In order to increase the usefulness of the table to this analysis and decrease its size, three acceptance criteria were applied to all entries:

- 1) The half-life of the activity must be at least five minutes; shorter lived activities are generally beyond the reasonable reach of our experiments;
- 2) The energy of the transition must be at least 90 keV; lower energy γ -rays are rejected from the spectral analysis for reasons previously discussed; and
- 3) The abundance of the transition must be greater than 0.5%; this is a criterion based on the empirical observation that such low intensity transitions are not observable in the complex γ -ray spectra that heavy-ion-induced reactions typically generate.

TABLE III. Decay curve component analysis options.

Number of components	Choice of half-lives to be used
Single component:	a) Known γ -ray transition from table. b) Straight line, graphically selected
Multiple components:	a) Known γ -ray plus constant background. b) Straight line plus constant background. c) Sum of two known γ -rays d) Sum of known γ -ray plus straight line. e) Sum of two straight lines, graphically selected. f) Growth of known γ -ray from its known parent.

4.2 Decay Curve Identification Criteria

Several criteria have been developed to aid in the rapid and accurate assignment of observed γ -ray decay curves. The correct and expedient recognition of a decay curve is important for the primary reason of lowering the interactive computer time and cost, and also to reduce the ultimate chore of generating a self-consistent set of assignments, particularly with regard to multiple assignments to a single decay curve. The first order criterion to aid in the assignment of an observed γ -ray decay is chemistry. On several occasions the target was separated into chemical fractions following irradiation [1,6,8,12]. Gamma-rays subsequently observed in the fractions had to be ascribed to nuclides with the proper chemical properties as well as γ -ray energy and half-life. To aid in this identification, the chemical fraction into which nuclides would be separated via the Kratz chemistry [7] is contained for these entries in the γ -ray table where it is known. The chemical separation greatly aids the identification of observed activities because the assignment is usually unique, i.e., only one candidate will meet the three criterion of chemistry, half-life, and γ -ray energy.

However, targets are not always chemically separated before spectrometric analysis; generally, the first time a given projectile-target system is studied the target would not be separated. This is to enable the experimenter to get an overview of the possible reaction products and their relative importance. Subsequent irradiations would then focus on the details of the reaction product distributions using chemical separation before γ -ray spectroscopy. In the former case no chemical information is available on the observed gamma-rays and the "live time identification" can only be made on the basis of half-life and gamma-ray energy. The consistency of the identifications with regard to multiple transitions is checked later by hand when all the decay curves have been identified. The earliest criterion adopted to aid in the reduction of the amount of time spent connected

to the main computer was the brute force method to accept all possible candidates with approximately the observed half-life and in the gamma-ray energy interval of ± 1 keV. Then multiple assignments were reviewed offline. After the analysis of many sets of nuclidic identifications of gamma ray spectra of unseparated targets, an empirical criterion has been established based on the absolute (or relative) abundances of the gamma-ray candidates. Simply stated, gamma-ray transitions that have abundances less than 5 percent are not observed, except if the nuclide is produced with an unusually high cross section or if there are very few radioactivities present. Examples of these exceptions are (1) products from few nucleon transfer between heavy ion reaction partners which can be produced with cross sections approximately ten times as large as other reaction products, and (2) targets from light ion bombardments such as $^3\text{H} + \text{natBaCl}_2$, where essentially the only radioactivities present were ^{140}Ba and ^{140}La [14]. Both of these exceptions are easily recognized and present no difficulty in application of this empirical criterion.

4.3 Cross Section Calculations

The first step in the compilation of the cross section data after completing the interactive decay curve fitting is to generate an energy-ordered list of cross sections, calculated for each accepted decay curve component. This list is important because it contains all the cases where more than one identification was made. However, these cases of multiple identifications are not resolved at this stage, they are only noted.

The cross sections are calculated for each component of every decay curve by using the A_0 and half-life information on the punched card output from TAU2 and using the well known equation for the cross section that encompasses fluctu-

ations in the beam intensity by dividing the bombardment into n short intervals:

$$\sigma = A_0/N \sum_{i=1}^n \phi_i (1-e^{-\lambda t_{bi}}) \left\{ \exp -\lambda \left(\sum_{j=i+1}^n t_{bj} \right) \right\} \quad (6)$$

where T_B (the total length of bombardment) is equal to the sum of the lengths of the n short intervals t_{bi} :

$$T_B = \sum_{i=1}^n t_{bi} \quad (7)$$

N is the number of target atoms, A_0 is the measured activity extrapolated to the end of bombardment, and ϕ_i is the beam flux during the i^{th} interval. It is convenient to use this expanded form of the cross section equation because very often the beam level during the bombardment of target materials will fluctuate and occasionally be interrupted for short periods of time.

After the energy-sorted list of identifications has been prepared, the TAU2 output cards are sorted by isotope and a second calculation of the cross section is performed for each gamma transition and weighted average cross sections are calculated for each isotope. It is at this point that all the decay curve identifications are screened. Generally the isotopic listing is used as a basis and each isotope is checked to make sure that:

- a) All the gamma-ray identifications were unique, i.e. that if a multiple assignment was made to a singular γ -ray transition, only one of the assignments is accepted as being correct. If no resolution is attainable then that γ -ray transition is thrown out.
- b) All the γ -ray transitions for a given isotope give consistent values for the production cross section of that isotope.

- c) The γ -ray transitions for a single nuclide are observed in the proper ratios when compared to their known abundances; i.e. no γ -ray lines with intensities stronger than or roughly equal to the weakest observed transition can be missing, unless they can be shown to be masked by a more intense gamma-ray. Also the energy of the observed γ -ray should be reasonably close to the literature value, typically ≤ 0.2 keV -- assignments with large deviations must be discarded.

This review of the identifications is accomplished through the use of the gamma ray table [4], the microfiche record of the decay curve fitting, and the listing of the cross section calculations by E_γ and isotope. A particularly troublesome group of radionuclides consists of those activities with only one strong (therefore only one observable) γ -ray transition. There is no consistency check for these activities other than the half-life and energy of the gamma-ray. Occasionally a pair of such activities are assigned to the same observed gamma-ray transition and there is no way a priori to choose between them. An example of such a pair is ^{148}Nd ($E_\gamma = 211.3$ keV, $T_{1/2} = 1.73$ hr) and ^{121}I ($E_\gamma = 212.5$ keV, $T_{1/2} = 2.12$ hr); observed as part of a two-component decay curve from an unseparated Eu target irradiated with an ^{56}Fe beam.

5. ERRORS IN CROSS SECTIONS

The uncertainties in the calculated cross sections are based on the uncertainty in the weighted average of the A_0 values from the fits to the decay curve. As was stated before, uncertainty in the measured efficiencies due to not exactly reproducing the measured geometry has been measured to be $\leq 4\%$ at the smallest detector-source distance used. The uncertainty in the peak

area determination with SAMPO has been discussed previously [3,10]. In order to reduce the amount of information transmitted between the segments of decay curve analysis, the decay curves are constructed with a 10% error assigned to each data point. This is, of course, an approximation that assumes that the peak areas of a given γ -ray transition contain approximately 100 counts. This is usually an overestimation of the error, but the assumption that the error is taken to be a constant fraction is not so bad because as the samples get weaker they are counted for progressively longer time intervals.

The uncertainties in the A_0 values are calculated as the statistical uncertainties in the coefficients, a_j , of a sum of exponential functions that has been fit to each decay curve. These uncertainties can be written as [15]:

$$\sigma (a_j)^2 \approx S^2 \epsilon_{jj} \quad (8)$$

where ϵ_{jj} is the diagonal element of the error matrix, obtained from the least square fitting routine, and S^2 is the sample variance for the fit of n exponential functions to N data points, y . This sample variance is written:

$$S^2 = \frac{1}{\nu} \sum_{i=1}^N \left\{ y_i - \sum_{j=1}^n \left[a_j e^{-\lambda_j t_i} \right] \right\}^2 \quad (9)$$

where ν is the number of degrees of freedom, $\nu = N - (n+1)$, λ_j is the mean life of the j^{th} component, and t_i is the midpoint in time of the i^{th} measurement.

This error in A_0 is then used via propagation of errors to give the error in the measured cross section for each identified gamma-ray transition. However, the uncertainty in the cross section for a nuclide which was identified by more than one γ -ray transition is calculated from the error in the weighted average cross section.

5.1 Misidentifications

Due to the stringent screening procedure used, the number of misidentified nuclides that have more than one observable γ -ray transition is very small, probably less than one per experiment. However, misidentifications do come from nuclides with only one gamma-ray transition because, as it turns out, such nuclei make up a large class spanning a wide range of half lives and γ -ray energies. Contributions from such misidentification have been estimated to be 1 in 50. Even though they are not recognizable at this stage of the analysis, they can usually be found through their incorrect behavior in the charge and mass distribution analysis. This will be discussed in a subsequent paper.

6. APPLICATIONS OF THE METHOD

A summary of the computer codes and their operating characteristics developed for the measurement of product yield cross sections from heavy-ion-induced nuclear reactions is given in Table IV. Up to the present the method has been used exclusively to study heavy ion nuclear reactions. The method has been applied to samples ranging from 51 mg/cm² U foils irradiated with relativistic projectiles at the Bevalac at LBL to a 34 mg/cm² Al foil irradiated with ⁹³Nb ions at the LBL SuperHILAC to a 0.5 g/cm² BaCl₂ target irradiated with ³H at Los Alamos Scientific Laboratory. The method has proven to be successful at extracting the cross sections (or activity levels) of gamma-ray-emitting nuclides from very complex γ -ray spectra, because measurement of gamma-ray spectra as a function of time allows the nearly unambiguous identification of product radionuclides through both their gamma-ray transition energies and half-life.

We believe the inclusion of the measurement of the latter quantity, the radioactivity's half-life, and its effective use in the identification scheme is the key ingredient in the system we have developed. While the method we have described is well suited, albeit necessary, for the study of the reaction products from heavy-ion-induced nuclear reactions, it also lends itself to the measurement of individual radioactive products when a large mix of species are present, such as neutron activation of terrestrial samples. In fact we have found that a great deal can be learned about the distribution of reaction products without resorting to radiochemical separations prior to gamma-ray spectroscopy.

Table IV. Summary of computer codes used in this work.

Code	Description	Compiled Execution Size (Octal words)	Machine Used	Running Time
SAMPO	Peak Search and Fitting	74000	CDC-7600	~4. CPU sec per complex spectra
TAU1	Peak Area Sorting for Decay Curve Construction	55000	CDC-7600	~0.2 CPU m sec per spectra per decay curve
TAU2	Decay Curve Identification (interactive)	37000	CDC-6400 and CDC-6600	
CRSPLT	Cross Section Calculation and Plotting	44000	CDC-7600	~10. CPU m sec per isotope

ACKNOWLEDGMENTS

As with any program that spans many years, the work described in this paper has benefitted from the ideas, critical review, and developmental efforts of many people. The authors would like to acknowledge J. O. Liljenzin who performed much of the ground work for the computer-based identification scheme, and M. M. Fowler, J.V. Kratz and A.E. Norris who helped to carry on this early work. Special thanks are also due to I. Binder, R. Kraus, R. Klein, and E. Dong who oversaw the compilation and updating of the γ -ray table that was essential to our identification process. Thanks also to B. V. Jarrett who worked with us to develop a computer-based multichannel analyzer system that made an automatic SAMPO analysis possible. We also wish to thank W. D. Loveland for his encouragement and critical review of our method.

This work was done with the support from the U.S. Department of Energy.

REFERENCES

- [1] R.J. Otto, M.M. Fowler, D. Lee, and G.T. Seaborg, *Phys. Rev. Lett.* 36, 185 (1976).
- [2] W. Loveland, R.J. Otto, D.J. Morrissey, and G.T. Seaborg, *Phys. Rev. Lett.* 39, 320 (1977).
- [3] J.T. Routti and S.G. Prussin, *Nucl. Inst. Meth.* 72, 125 (1969).
- [4] I. Binder, R. Kraus, R. Klein, D. Lee, and M.M. Fowler, Lawrence Berkeley Laboratory Report LBL-6515 (1977).
- [5] W.W. Bowman and K.W. MacMurdo, *Atomic and Nuclear Data Tables* 13, 89 (1974).
- [6] W. Loveland, D.J. Morrissey, R.J. Otto, and G.T. Seaborg, Lawrence Berkeley Laboratory Report LBL-6527 (1977).
- [7] J.V. Kratz, J.O. Liljenzin, and G.T. Seaborg, *Inorg. Nucl. Chem. Letters* 10, 951 (1974).
- [8] See, for example, M. de Saint Simon, R.J. Otto, and G.T. Seaborg, Lawrence Berkeley Laboratory Report LBL-7114, *Phys. Rev. C*, submitted for publication.
- [9] SRM-4216-C is a standard reference material available from National Bureau of Standards, Washington, D. C.
- [10] J.T. Routti, Lawrence Berkeley Laboratory Report UCRL-19452 (1969).
- [11] I. Binder, University of California, Berkeley, Ph.D. Thesis, Lawrence Berkeley Laboratory Report LBL-6526 (1977).
- [12] J.V. Kratz, J.O. Liljenzin, A.E. Norris, and G.T. Seaborg, *Phys. Rev.* C13, 2347 (1976).
- [13] W. Loveland, R.J. Otto, D.J. Morrissey, and G.T. Seaborg, *Phys. Lett.* 69B, 284 (1977).
- [14] C. Detraz, private communication (1977).
- [15] P.R. Bevington, Data Reduction and Error Analysis for the Physical Sciences (McGraw-Hill, New York 1969), p. 153.

FIGURE CAPTIONS

- Fig. 1. Computer programs used for automatic and interactive Data Analysis
(A) Automatic mode, peak analysis and decay curve construction.
(B) Interactive mode, decay curve analysis.
- Fig. 2. Typical nonlinearity of the gamma-ray spectrometers used in this work. The nonlinearity is taken to be the difference between a linear and a polynomial fit to the energy calibration data.
- Fig. 3. Set of gamma-ray detector efficiency curves for the various standard geometries of system Ge(Li)-3.
- Fig. 4. Measured two gamma-ray cascade sum peak as a function of source-detector distance for system Ge(Li)-3 for a ^{94}Nb source.
- Fig. 5. Typical results of the variation of the fitted full width at half maximum (FWHM) in keV as a function of gamma-ray energy.
- Fig. 6. Typical gamma-ray spectrum observed in this work. A gold target was irradiated with 1140-MeV ^{136}Xe ions and the gamma radiation measured directly [11]. The energy range of the measurement was 75 to 2000 keV in a 4096-channel spectrum. (XBL 776-8998)
- Fig. 7. Schematic block diagram of the computer program TAU2.
- Fig. 8. Graphics terminal display showing the fit of a single component (^{123}I , solid line) to the measured decay curve of a 159.3 keV gamma-ray (open circles). The ordinate is the logarithm of the count rate and the abscissa is the time after and of bombardment in days. Also shown on the CRT display are 20 gamma-rays, nearest in energy to the measured 159.3 keV, from the Binder et al. gamma-ray catalogue.⁴ These entries, numbered A through T, contain information on the energy, chemical properties, isotope, half-life in days, percent abundance of the transition and chemical symbol of the parents, if any. (XBL 784-8222)

Fig. 9. Graphics terminal display, similar to Fig. 8, showing the fit of two components, ^{129}Ba and ^{82}Br , to the measured decay curve of a 1044.6 keV gamma-ray. (XBL 784-8228)

Fig. 10. Graphics terminal display, similar to Figs. 8 and 9, showing the fit of the growth of ^{135}Xe to the measured data.

COMPUTER PROGRAMS USED FOR AUTOMATIC AND INTERACTIVE DATA ANALYSIS

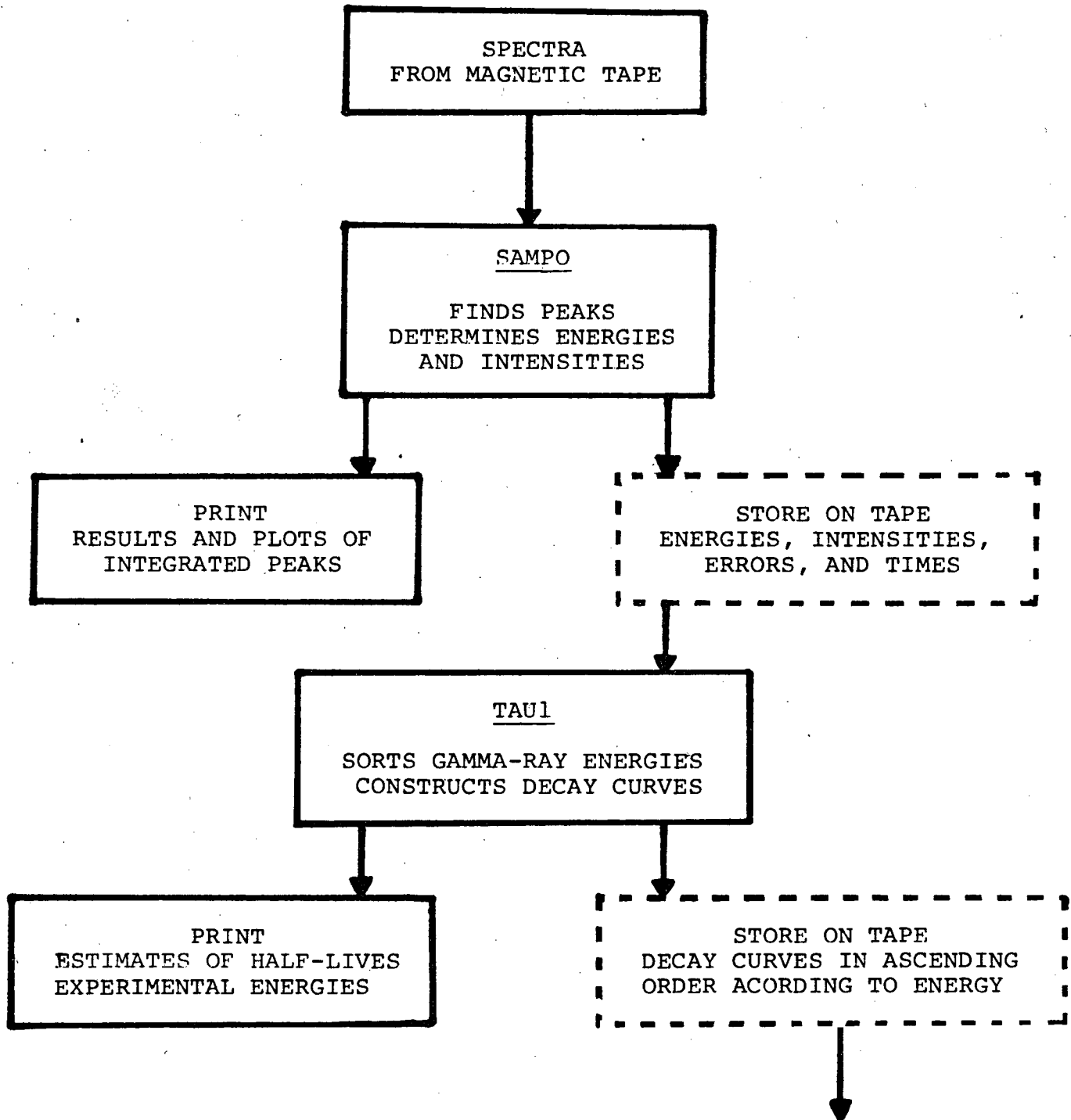


Fig. 1

(A) AUTOMATIC MODE: PHOTOPEAK ANALYSIS, AND DECAY CURVE CONSTRUCTION

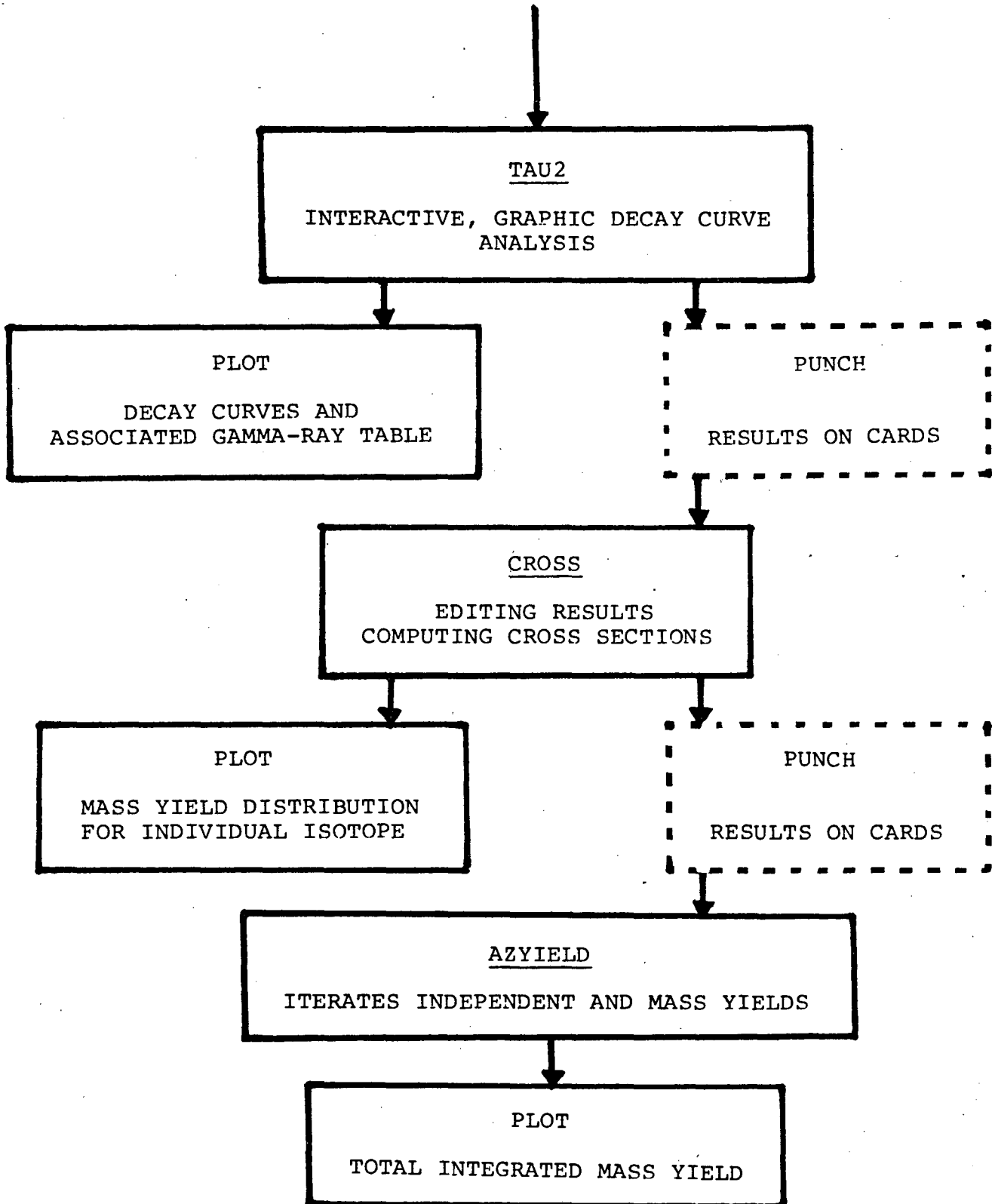
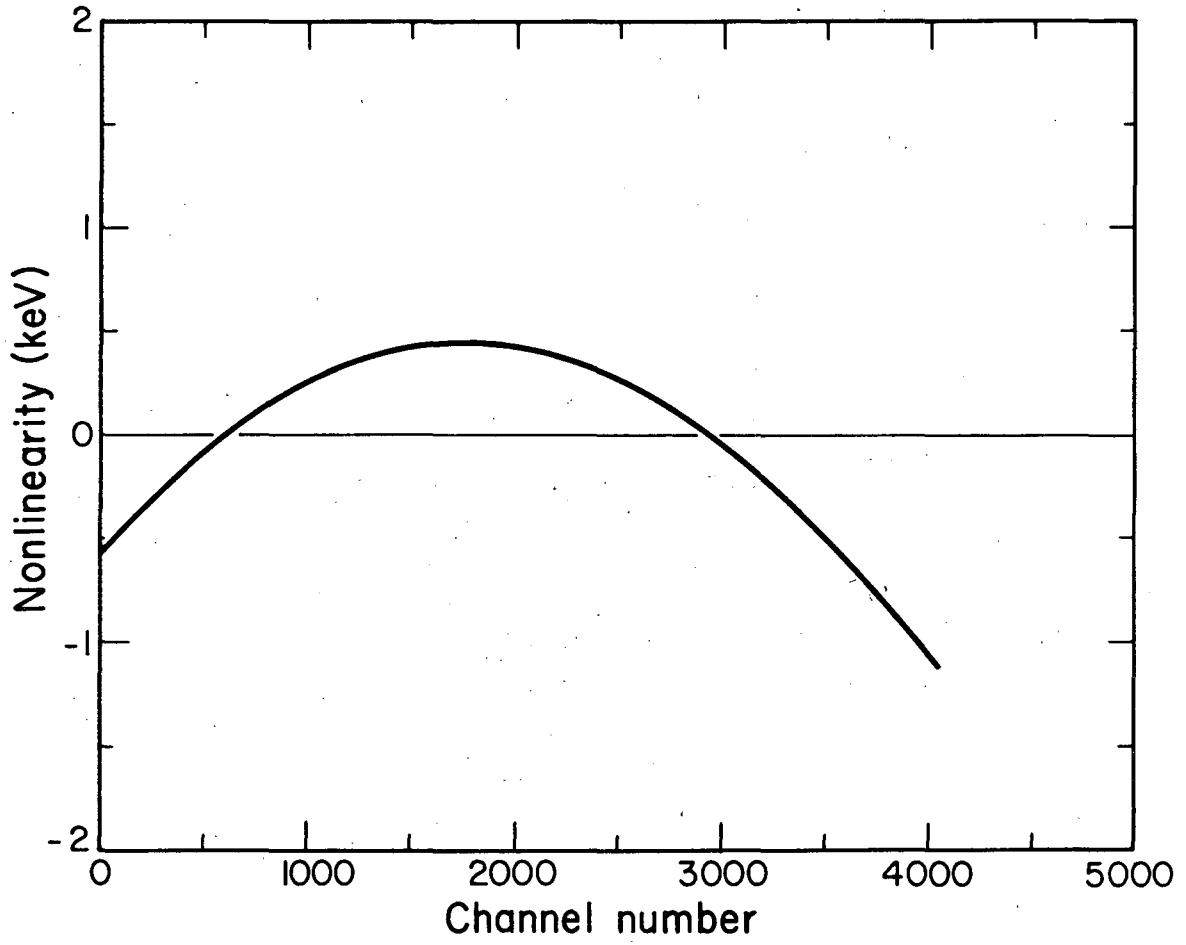


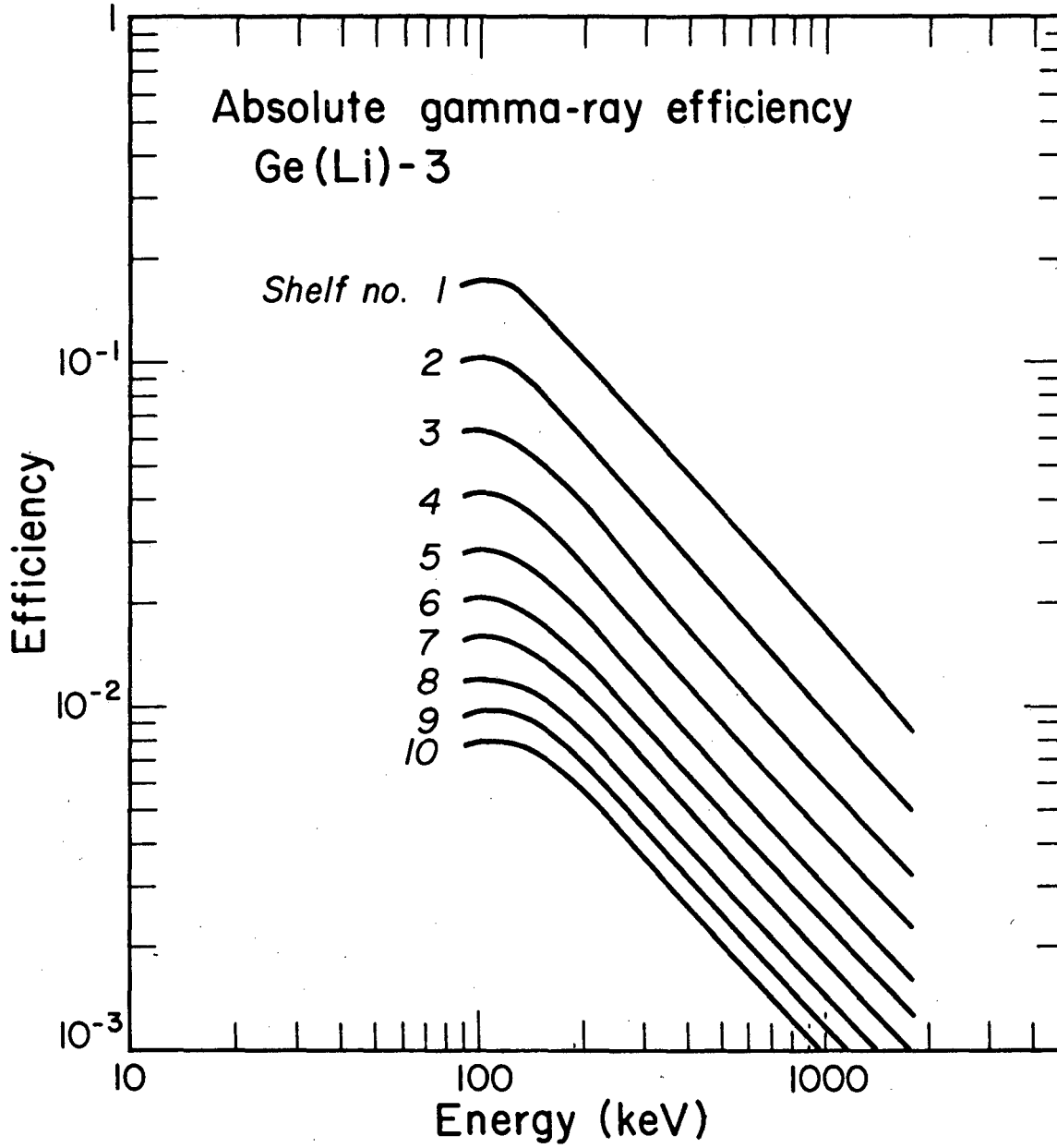
Fig. 1

(B) INTERACTIVE MODE: DECAY CURVE ANALYSIS, AND A TOTAL CROSS SECTIONAL YIELD CALCULATION



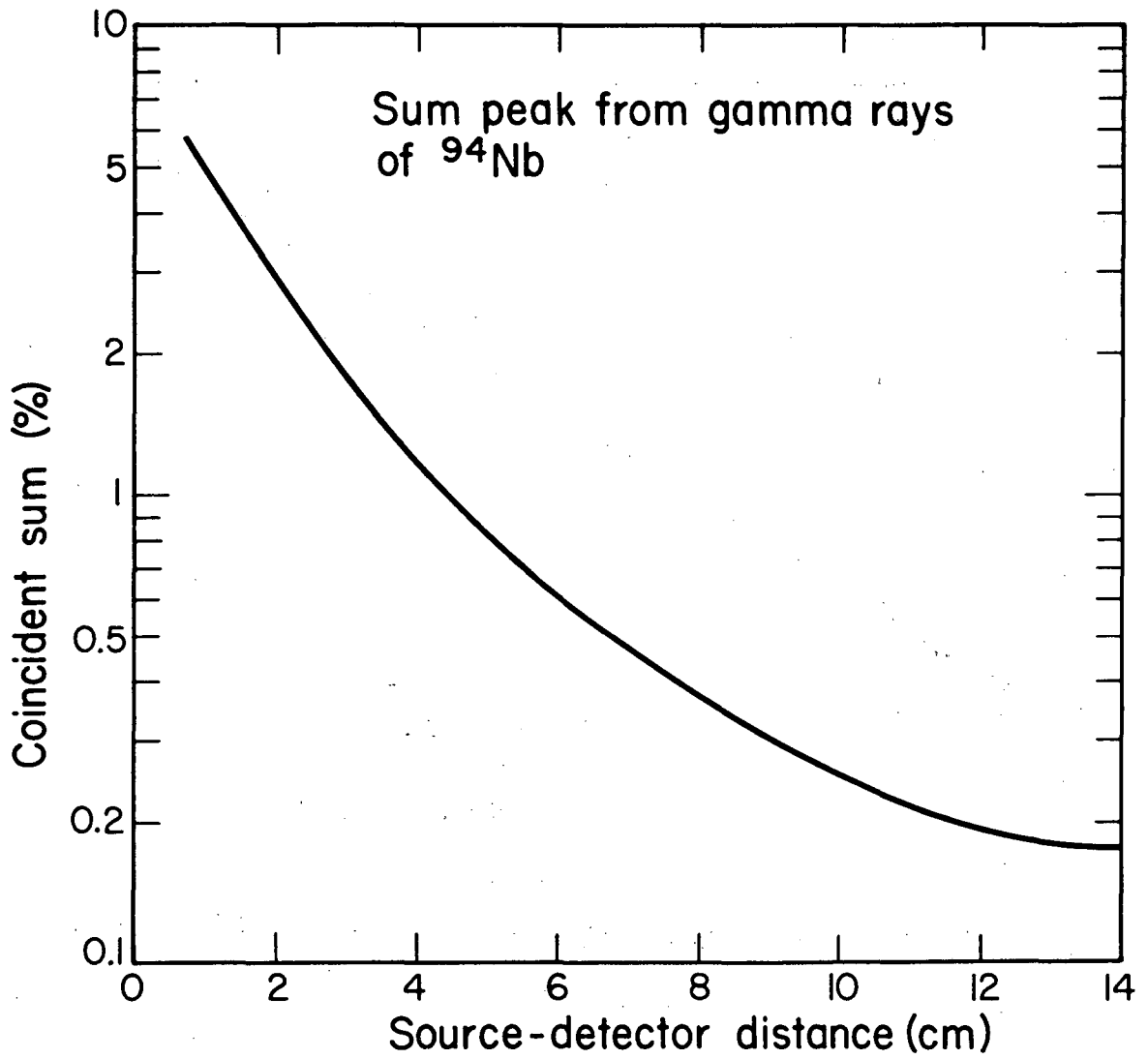
XBL 787-1376

Fig. 2



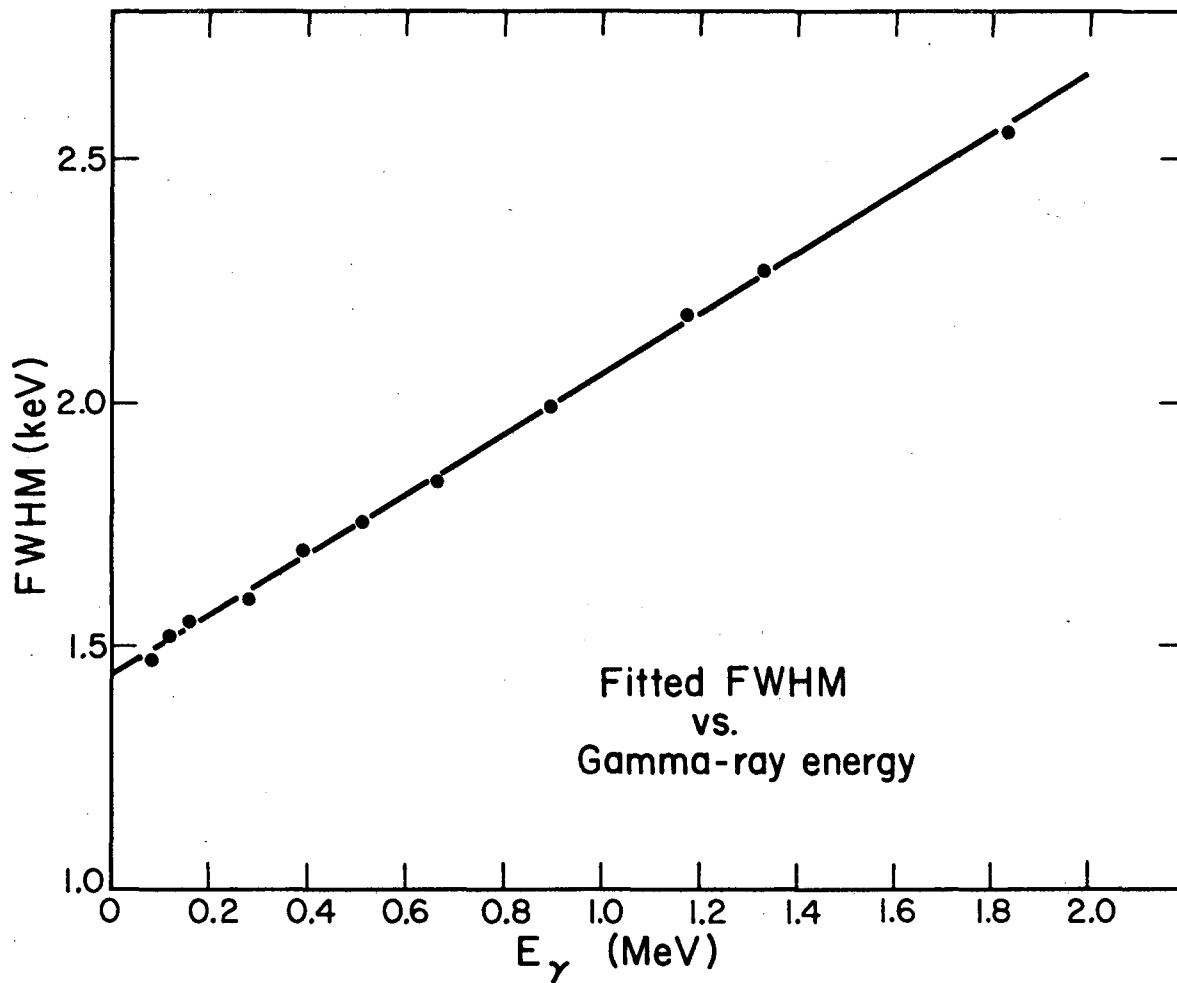
XBL 787-1374

Fig. 3



XBL 787-1377

Fig. 4



XBL 787-1375

Fig. 5

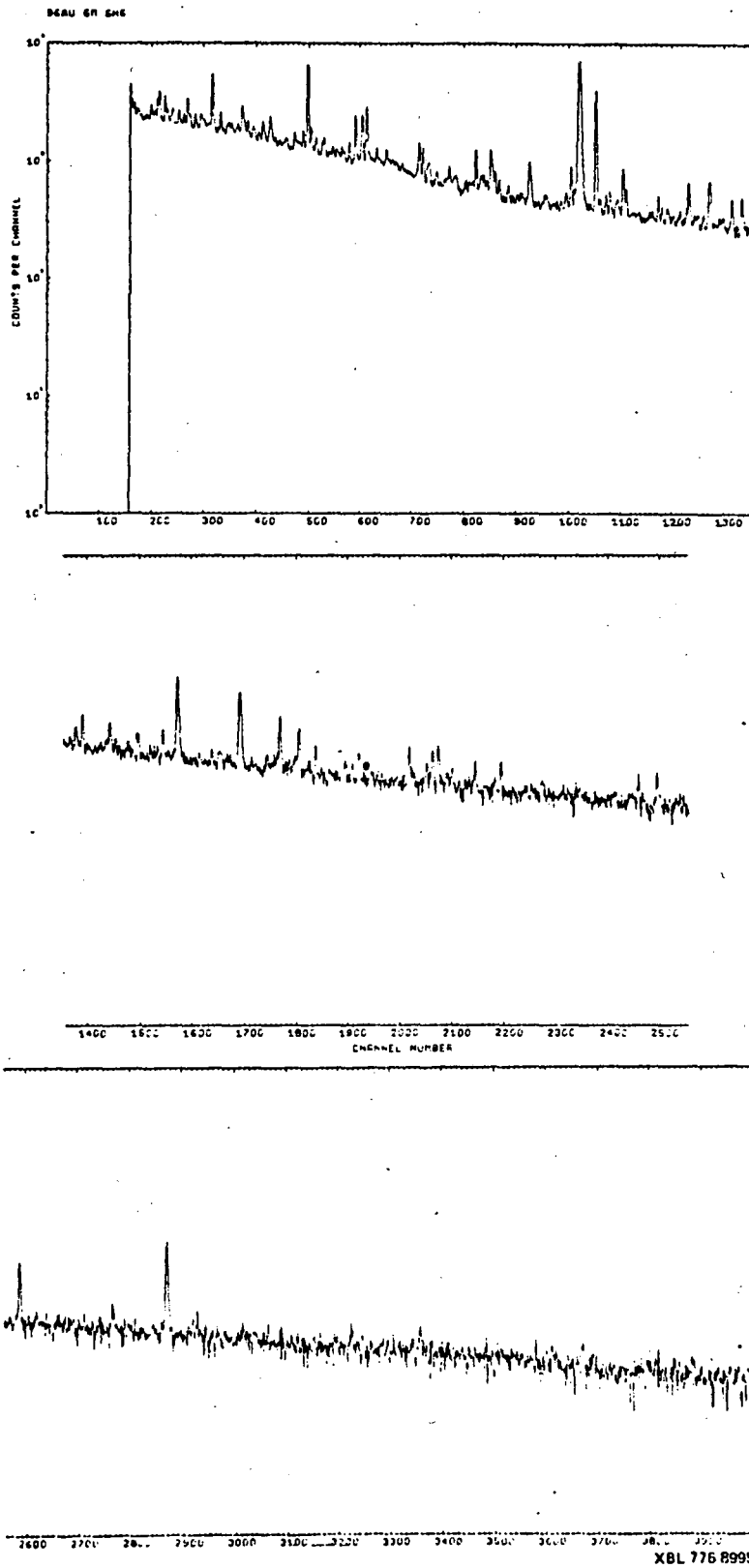
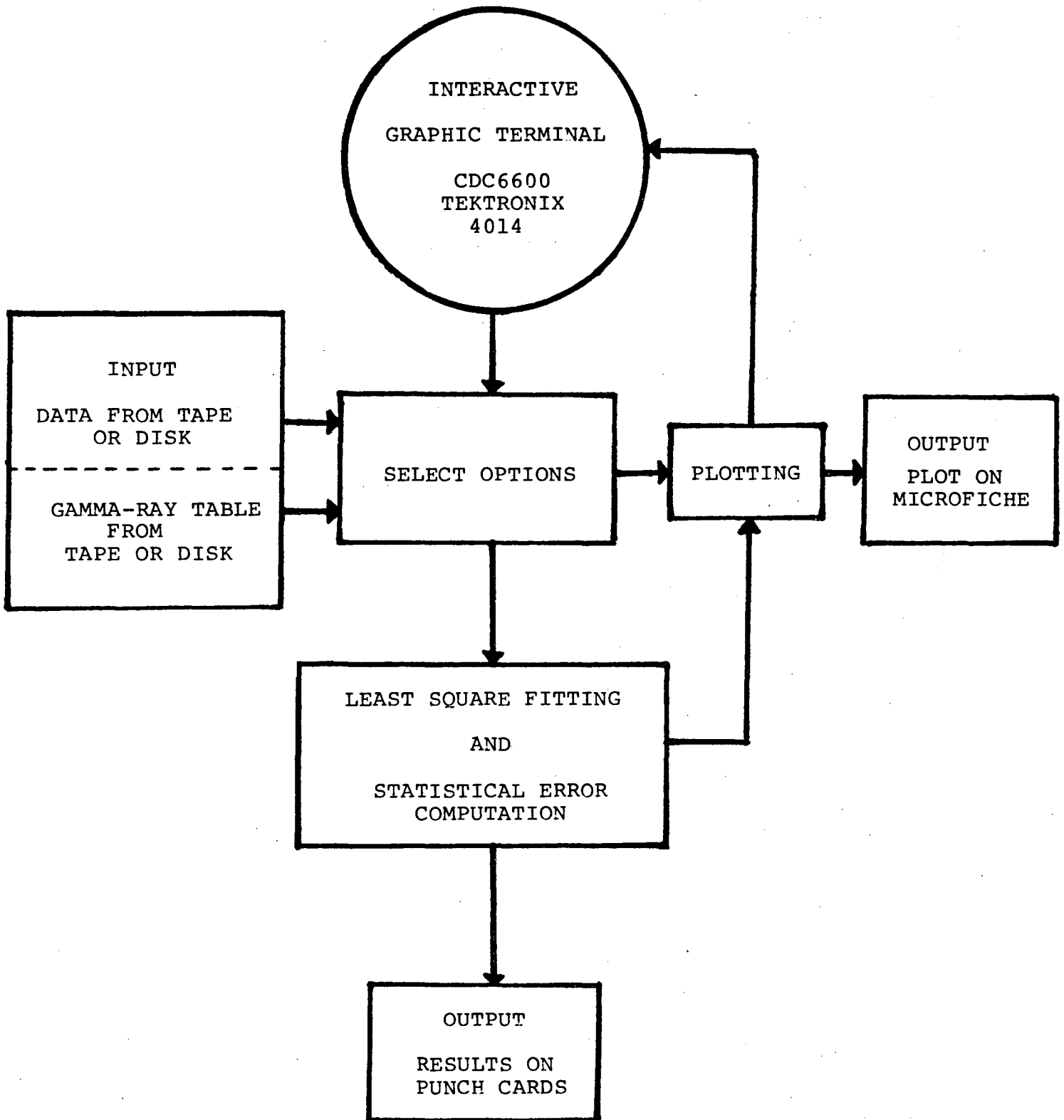


Fig. 6



SCHEMATIC BLOCK DIAGRAM OF THE COMPUTER PROGRAM TAU2

Fig. 7

1251

159.3KEV

159.1 I I -123

.546

(A) 158.5	DI SB-117	.117	87.0	TE	(K) 159.4	LA HO-159	.023	.6	ER
(B) 158.6	PB IN-117M	.081	17.0	CD CD	(L) 159.8	LA LU-177M	155.000	.6	
(C) 158.6	PB IN-117	.031	86.7	CD CD	(M) 159.8	LA EU-159	.013	1.5	
(D) 158.7	LA RA-223	11.400	.7	TH FR	(N) 159.8	LA GD-159	.013	1.4	
(E) 158.8	SH AU-191	.133	3.7	HG	(O) 160.2	LA NP-236	999.999	27.6	NP
(F) 158.8	SH PD-100	3.630	1.3	AG	(P) 160.3	I RN-223	.030	14.0*	
(G) 159.0	DI TE-123M	119.000	84.1		(Q) 160.3	DI SN-123M	.028	99.9	
(H) 159.1	I I -123	.546	83.0	XE	(R) 160.4	SH TA-173	.154	6.5	W
(I) 159.1	SH TC-105	.005	7.5		(S) 160.5	SH RE-183	71.000	.7	OS OS
(J) 159.4	LA SC- 47	3.410	73.0	CA	(T) 160.5	LA TB-155	5.600	3.2	DY

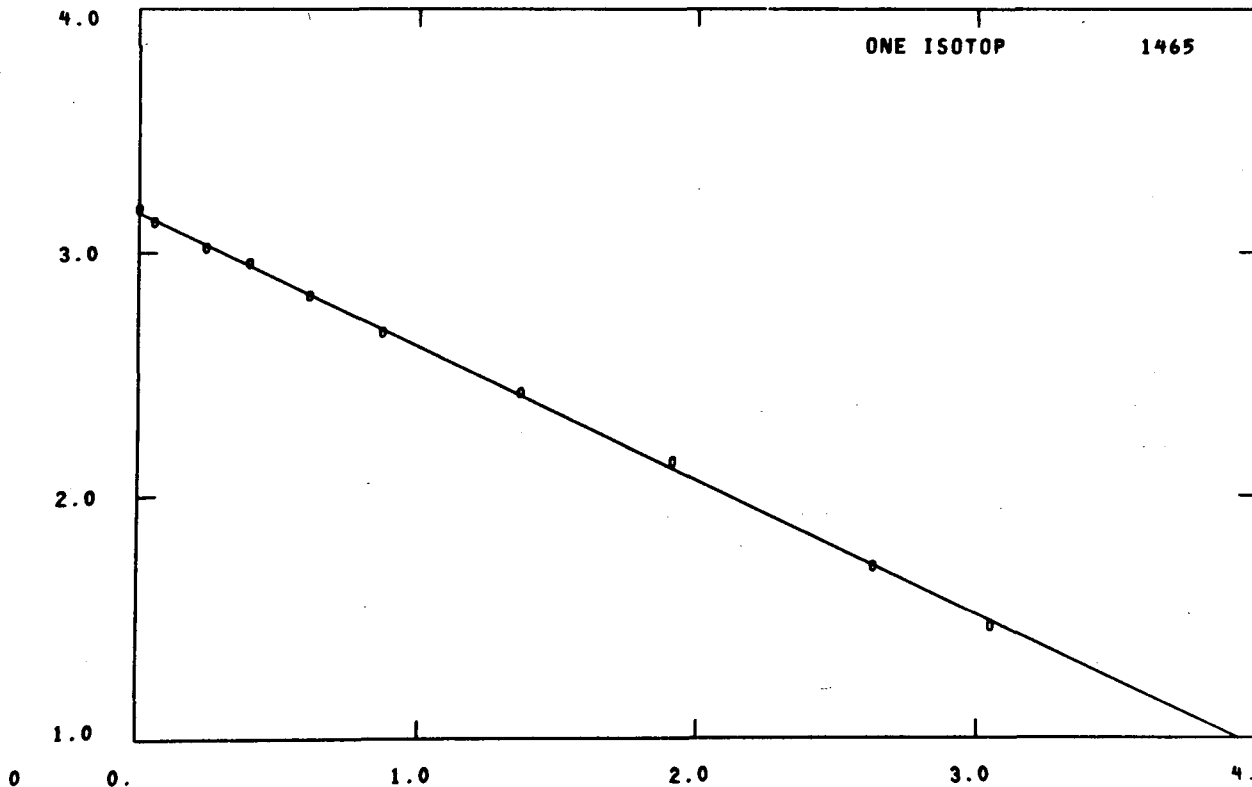


FIG. 8

XBL 784-8222

34AU

1044.6KEV

1044.7 LA BA-129
1043.9 I BR- 82

.096
1.479

(A)1041.9 LA GD-145	.017	10.1	GD	(K)1045.0 SH IR-186M	.073	.7	
(B)1043.4 SH CD-105	.038	.7	IN	(L)1045.1 LA SB-124	60.200	1.8	SB
(C)1043.7 LA EU-159	.013	.5		(M)1045.4 LA TB-150A	.136	1.2	DY HO
(D)1043.7 LA LA-142	.066	2.8	BA	(N)1045.7 SH AG-106M	8.410	29.7	
(E)1043.8 SH BI-205	15.300	4.9	PO AT	(O)1046.0 LA FR-212	.013	13.7	
(F)1043.9 I BR- 82	1.479	27.8	BR	(P)1046.3 SH TC-102	.003	11.5	MO
(G)1044.1 PB RB- 82M	.258	33.2		(Q)1046.4 LA SM-141	.007	1.5	
(H)1044.4 LA EU-156	15.190	.5	SM	(R)1046.4 SH AU-188	.006	1.4*	
(I)1044.6 SH IR-184	.129	5.8	PT	(S)1046.6 LA LA-132M	.017	5.6	
(J)1044.7 LA BA-129	.096	16.0*		(T)1046.6 LA RH-102M	999.999	34.0	

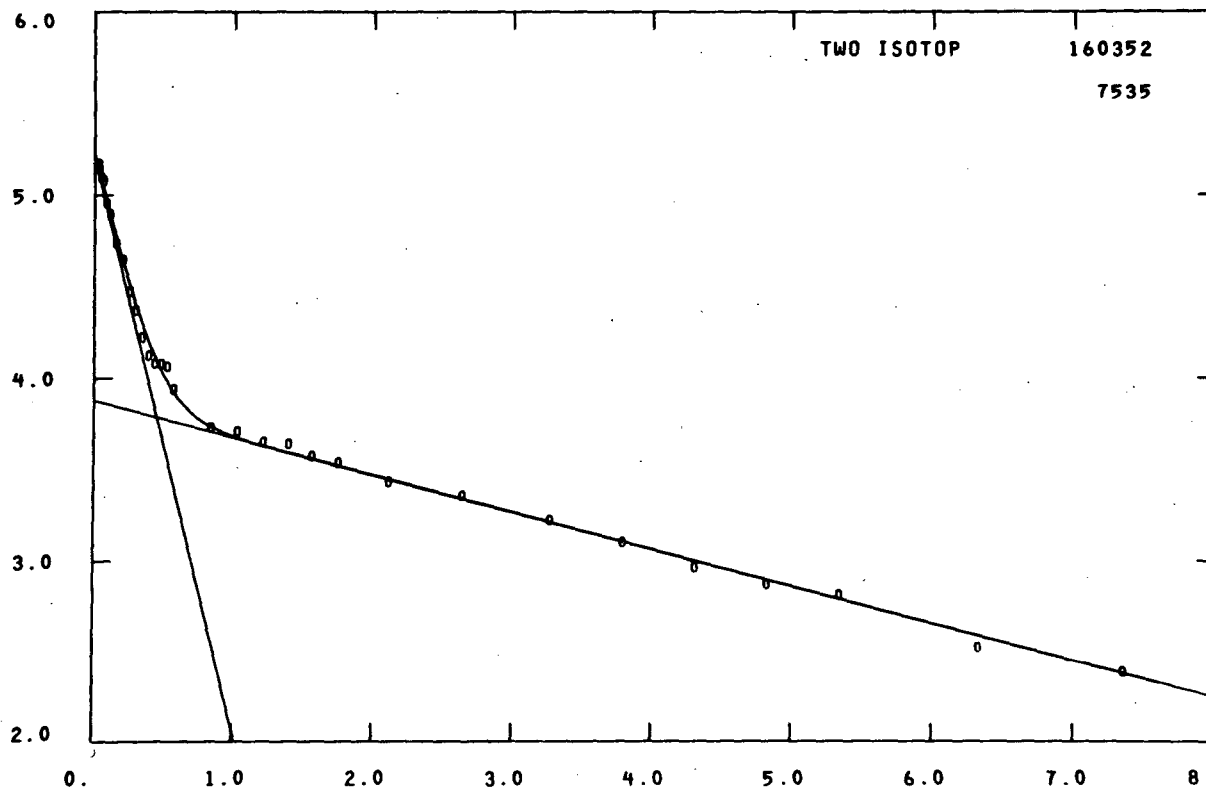


Fig. 9

XBL 784-8228

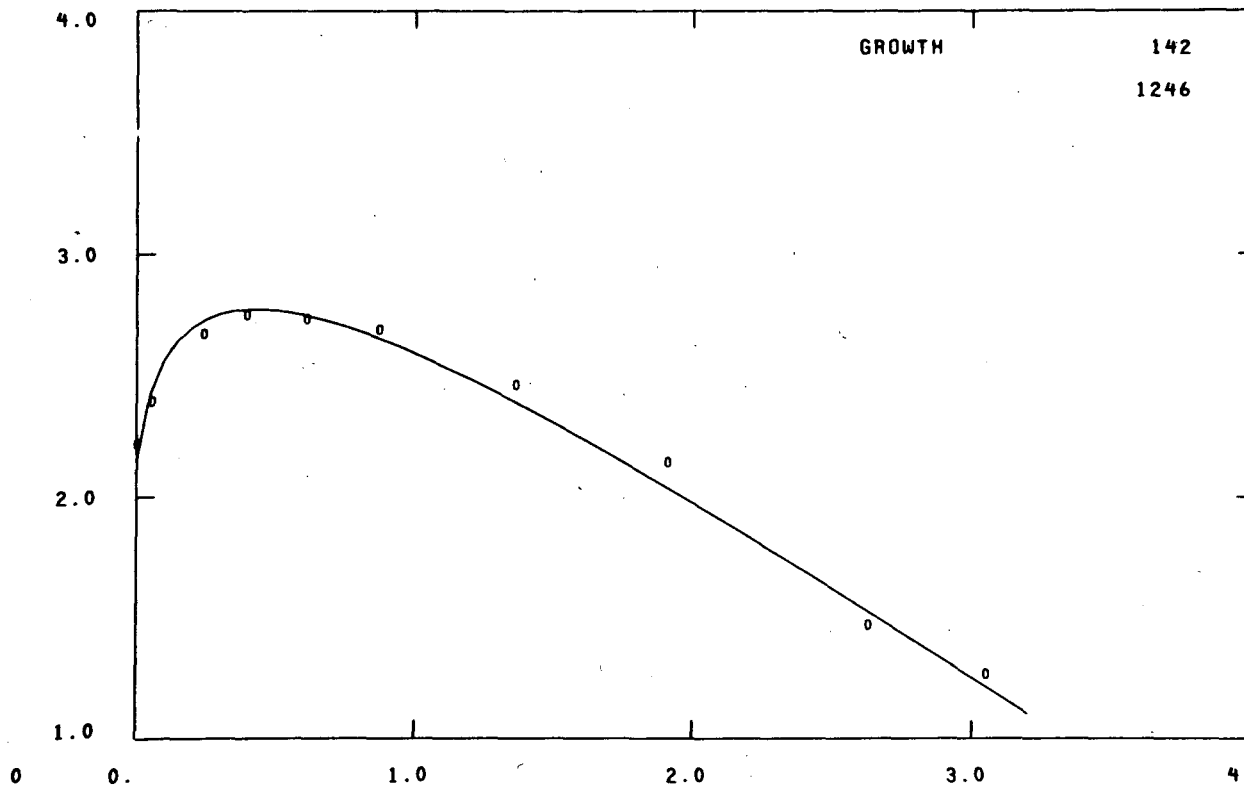
125I

250.1KEV

249.6 I XE-135 .382
249.6 I XE-135 .382

(A) 248.5 LA LU-166	.002	4.8*	HF	(K) 250.1 LA ND-152	.008	21.0
(B) 248.5 LA CE-133	.225	2.5	PR	(L) 250.3 I CL-39	.039	47.1
(C) 248.8 LA PA-234	.281	2.5	PA	(M) 250.6 SH IR-183	.040	2.5*
(D) 248.9 6A TM-165	1.233	.8	YB	(N) 250.8 LA TB-163	.014	7.0
(E) 249.4 LA BA-131	11.700	1.5	LA	(O) 250.9 LA CE-146	.010	3.5 LA
(F) 249.6 SH PO-207	.237	1.8	RN AT	(P) 251.4 SH AU-187	.006	66.0
(G) 249.6 I XE-135	.382	92.0	I XE	(Q) 251.5 PB NP-240M	.005	1.0 U
(H) 249.7 LA SB-128	.371	.6	SN	(R) 251.5 LA CE-132	.175	2.6
(I) 249.7 I BR-77	2.375	3.3	KR BR	(S) 251.6 SH IR-195M	1.750	1.9 OS
(J) 250.1 I RN-211	.608	10.0		(T) 251.8 LA RH-97	.031	1.2 RH

FIG. 10



XBL 784-8223

This report was done with support from the Department of Energy. Any conclusions or opinions expressed in this report represent solely those of the author(s) and not necessarily those of The Regents of the University of California, the Lawrence Berkeley Laboratory or the Department of Energy.

TECHNICAL INFORMATION DEPARTMENT
LAWRENCE BERKELEY LABORATORY
UNIVERSITY OF CALIFORNIA
BERKELEY, CALIFORNIA 94720